

1 Early root phenotyping in sweetpotato (*Ipomoea batatas*
2 L.) uncovers insights into root system architecture
3 variability
4

5 Luis O. Duque¹
6

7 ¹Department of Plant Science, The Pennsylvania State University, University Park, PA 16802,
8 USA
9

10 Corresponding Author:

11 Luis Duque¹

12 109 Tyson Building, University Park, 16802, USA

13 Email address: lud88@psu.edu
14

15 **Abstract**

16 **Background.** We developed a novel, non-destructive, expandable, ebb and flow soilless
17 phenotyping system to deliver a capable way to study early root system architectural traits in
18 stem derived adventitious roots of sweetpotato (*Ipomoea batatas* L.). The platform was designed
19 to accommodate up to 12 stems in a relatively small area for root screening. This platform was
20 designed with inexpensive materials and equipped with an automatic watering system.

21 **Methods.** To test this platform, we designed a screening experiment for root traits using two
22 contrasting sweetpotato genotypes, ‘Covington’ and ‘NC10-275’. We monitored and imaged root
23 growth, architecture, and branching patterns every five days up to 20 days.

24 **Results.** We observed significant differences in both architectural and morphological root traits
25 for both genotypes tested. After 10 days, root length, surface root area, and root volume were
26 higher in ‘NC10-275’ compared to ‘Covington’. However, average root diameter and root
27 branching density were higher in ‘Covington’.

28 **Conclusion.** These results validated the effective and efficient use of this novel root
29 phenotyping platform for screening root traits in early stem-derived adventitious roots. This
30 platform allowed for monitoring and 2D imaging root growth over time with minimal
31 disturbance and no destructive root sampling. This platform can be easily tailored for abiotic
32 stress experiments, permit root growth mapping and temporal and dynamic root measurements of
33 primary and secondary adventitious roots. This phenotyping platform can be a suitable tool for
34 examining root system architecture and traits of clonally propagated material for a large set of
35 replicates in a relatively small space.
36

37 **Subjects**

38 Plant Science, Agricultural Science
39

40 **Keywords**

41 Root phenotyping, sweetpotato, *Ipomoea batatas*, adventitious roots, root system architecture,
42 root branching density
43
44

45 Introduction

46 Crop productivity is mainly influenced by environmental factors which include, but are not
47 limited to fluctuating temperatures, seasonal radiant energy, available and accessible soil
48 moisture and mineral nutrients that are distributed in soil. Of the abovementioned factors, soil
49 moisture and mineral nutrients directly affect growth and distribution of root systems
50 ([Purushothaman et al., 2017b](#); [Purushothaman et al., 2017a](#); [Siddique et al., 2015](#); [Gao and](#)
51 [Lynch, 2016](#); [Burridge et al., 2016](#); [Zhan and Lynch, 2015](#)). Examining *in situ* or *ex situ* root
52 systems are key to understanding crop productivity, as soil resources are heterogeneously
53 dispersed in soil profiles or are prone to localized depletion, making root spatial growth and
54 distribution shape the capacity of a plant to capitalize on available resources ([Lynch, 1995](#)).
55 Research on improving root system architecture (RSA) under low nutrient, low input agriculture
56 and water stress could improve overall crop yield ([Wasson et al., 2012](#); [Kuijken et al., 2015](#)) and
57 favorable changes in root architecture for nutrient capture and utilization of soil moisture could
58 influence overall biomass accumulation, hence, yield ([Hammer et al., 2009](#); [Anami et al., 2015](#);
59 [Xie et al., 2017](#)). However, the exploration of RSA traits is laborious due to the impediment of
60 accessing the soil matrix.

61
62 To circumvent this constraint, numerous real-time growth monitoring systems have been
63 developed for root visualization and quantification with support of innovative optical recording
64 techniques used in greenhouse settings. Furthermore, newer methodologies and improvements on
65 existing platforms for phenotyping large number of genotypes, replicates and treatments are
66 being developed with more reliable results ([Kuijken et al., 2015](#); [Chen et al., 2011](#)). These *ex-*
67 *situ* root phenotyping platforms can be categorized into two broad groups: 1) soil/substrate
68 systems and 2) non-soil systems. The soil/substrate system consists of a rhizotron/-box/-
69 mesocosm containing sand, natural soil or artificial soil mix where root growth is either monitored
70 non-invasively with the use of X-ray micro-tomography, magnetic resonance imaging or CT
71 scanning or destructively by digging, removing and cleaning whole root system and afterward,
72 scanning and/or taking a picture for further analysis ([Nagel et al., 2012](#); [Blossfeld et al., 2011](#);
73 [Rascher et al., 2011](#); [Metzner et al., 2015](#); [Pflugfelder et al., 2017](#); [Saengwilai et al., 2014](#); [Zhan](#)
74 [et al., 2015](#)). The soilless systems include: hydroponics ([Clark et al., 2013](#); [Pace et al., 2014](#)),
75 agar or gellan gum ([Fang et al., 2009](#); [Iyer-Pascuzzi et al., 2010](#); [Clark et al., 2011](#); [Topp et al.,](#)
76 [2013](#); [Ribeiro et al., 2014](#)), aeroponics ([de Dorlodot et al., 2007](#); [Gaudin et al., 2011](#)), grow
77 pouches ([Hund et al., 2009](#); [Adu et al., 2014](#)), transparent soil ([Downie et al., 2012](#)) and
78 rhizoslides ([Le Marie et al., 2016](#)). Both *ex situ* systems present advantages as well as
79 disadvantages dependent on end results. For example, environmental unpredictability can be
80 reduced using standardized artificial media, nutrient composition and/or application and micro-
81 environment control of both systems. In addition, they have the capability of real-time direct root
82 growth observations avoiding destructive harvest and can be very high throughput. On the other
83 hand, the 2D or 3D nature of both systems force root growth and development in an unnatural
84 physical realm as well as in a chemically artificial media. Lastly, both systems have the
85 limitation of using seed and seedling growth as proxies for mature plants. Thus, the optimal
86 phenotyping platform should accommodate a range of desirable properties, such as, low
87 operating and developmental costs and the possibility of measuring large number of plants,
88 replicates and/or treatments ([Kuijken et al., 2015](#)). Up to now, the majority of techniques
89 developed for RSA phenotyping rely on the use of seedlings and early stage root phenotypes
90 which have shown some predictive value for later developmental stages ([Tuberosa et al., 2002](#)),

91 however other studies have shown that this is not the case when seedling root phenotypes are
92 compared to a mature plant ([Watt et al., 2013](#)), hence, a flexible phenotyping system that would
93 allow a time-series capture of several developmental stages would be of paramount importance
94 and have increased agronomic relevance. Now, there is a lack of a suitable root phenotyping
95 method enabling the study of time-series stem derived storage root systems for that is
96 inexpensive, scalable, and adoptable by low resource or fund-limited laboratories worldwide.
97 Here, we focused on the root system of the storage root crop, sweetpotato (*Ipomoea batatas* L.),
98 an important and emerging crop for both developing as well as for developed nations worldwide.
99

100 Sweetpotato, is a vegetatively propagated true root crop that provides food security for resource-
101 poor small holder farmers in Sub-Saharan Africa as well as in other tropical and sub-tropical
102 countries worldwide ([Khan et al., 2016](#)). Limited literature is available on sweetpotato root
103 growth and development when compared to cereals, and what is available, focuses on storage
104 root growth, bulking and yield leaving out RSA entirely. Sweetpotato roots are adventitious roots
105 (AR) originating from the shoot or underground stem ([Khan et al., 2016](#)), contrary to the root
106 systems of seed propagated crops which consist of embryonic primary roots, seminal roots and
107 stem borne crown roots ([Hochholdinger et al., 2004](#); [Hund et al., 2011](#)). Sweetpotato RSA is
108 composed of AR, lateral roots (LR) and storage roots (SR). The simple identification of a main
109 AR axis and emerging LR through spatial and temporal events would enable novel research to
110 further recognize mechanisms involved in LR emergence and function([Khan et al., 2016](#)). To
111 exploit early sweetpotato root traits as potential selection criteria for breeding programs that
112 target different environmental scenarios, attempts have to be guided towards the development of
113 1) a robust and reproducible root phenotyping platform, 2) sustain stem and root growth until
114 storage initiation, 3) express high heritability and/or repeatability for a given trait, 3) minimize
115 genotype x environment interaction, 4) be able to be used all year around, and 5) not be labor
116 intensive.

117
118 In our study, first we describe a novel, non-destructive, expandable, ebb and flow soilless
119 phenotyping platform that is equipped with a customized imaging setup for stem derived (i.e.,
120 ‘slips’) storage root systems using germination paper that is preferred for large scale root
121 phenotypic screens. And second, we examine the inherent genetic variations in root traits among
122 a commercially available sweetpotato clone and an unreleased breeder line. This system enables
123 the analysis of large number of replicates with relatively low-cost materials, non-destructive real-
124 time direct root growth observations and imaging based on RGB photography and WinRhizo
125 root image analysis.

126

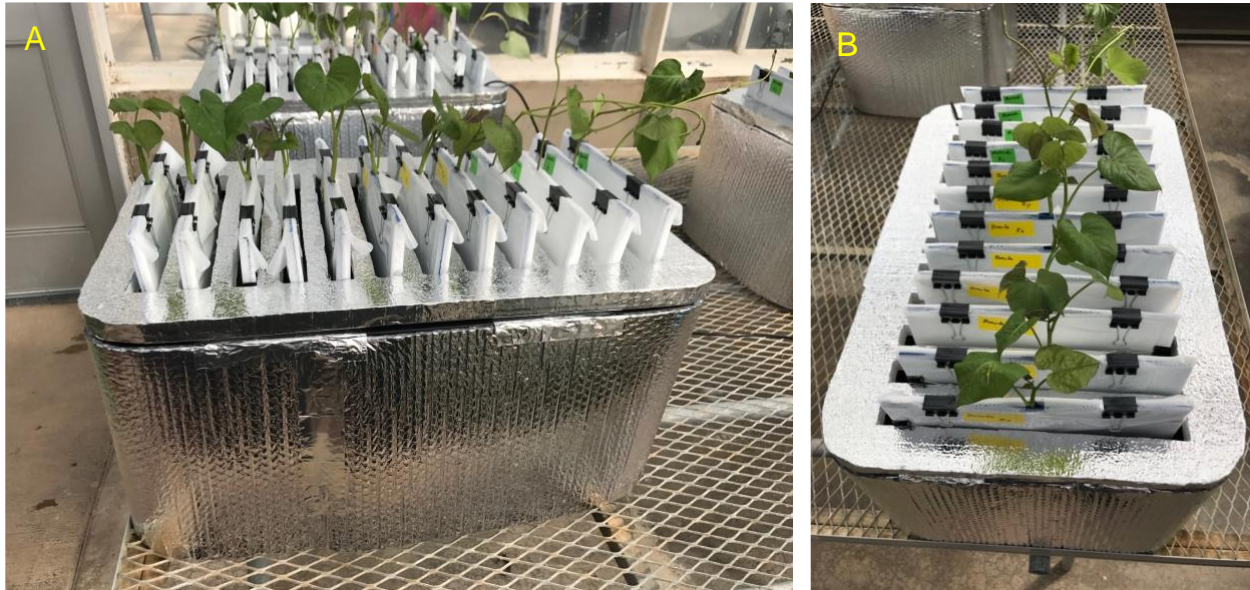
127 **Materials & Methods**

128

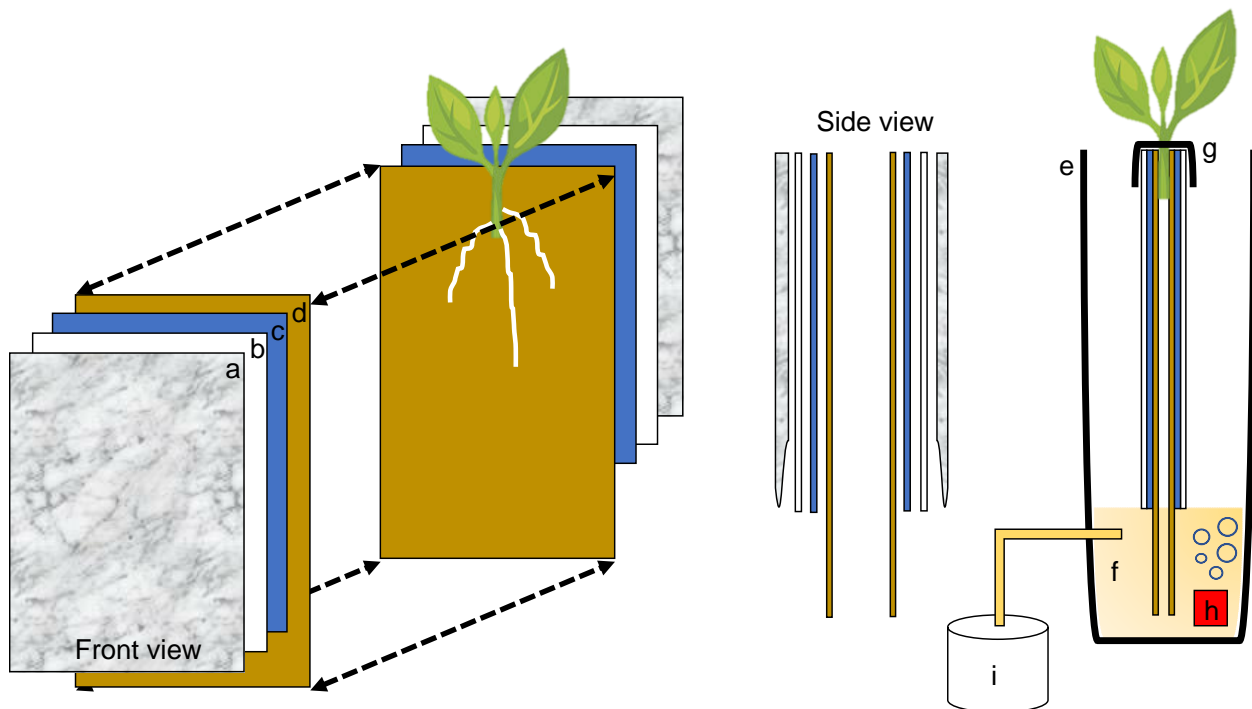
129 **Root phenotyping platform**

130 Each individual phenotyping system consisted of a 17-gallon (64.3 liter) heavy duty
131 polypropylene tough tote (26.88 in. L x 18 in. W x 12.5 in. H, HDX Model#
132 SH17GTOUGHTLDBY, Home Depot, Atlanta, GA, U.S.A.) protected with a radiant barrier
133 with a reflectance (IR) estimated at 94%+ (Reflectix Insulation, Markleville, IN, U.S.A.) (Figure
134 1A). The radiant barrier was used to prevent the phenotyping system from overheating caused by
135 direct natural and artificial light. The original plastic top lid was removed and a retrofitted
136 polyisocyanurate rigid foam insulation (Rmax Thermasheath-3, Dallas, TX, U.S.A.) was used in

137 its place. The retrofitted foam insulation lid was cut with 12 rectangular openings (13 in. L x 1
138 in. W spaced 1 in. apart from opening to opening) to accommodate each individual growth unit
139 (Figure 1B). Figure 2 shows a schematic representation of each phenotyping individual system.
140



141
142 Figure 1. Sweetpotato ebb and flow soilless phenotyping platform constructed and tested for stem-
143 derived adventitious roots: (A) side and (B) aerial view showing the 12 individual growth units fitted with
144 sweetpotato 'slips'.
145
146



147
148 Figure 2. Schematic representation of the semi-hydroponic ebb and flow phenotyping system: (a)
149 transparent plastic sheeting, (b) corrugated white plastic, (c) anchor steel blue seed germination paper,
150

151 (d), brown heavy weight germination paper, (e) tank or reservoir (not drawn to scale), (f), nutrient solution,
152 (g) securing clip, (h) bubbler, (i) nutrient tank retrofitted with an automatic submersible pump through a
153 time controller.

154

155 **Individual growth unit**

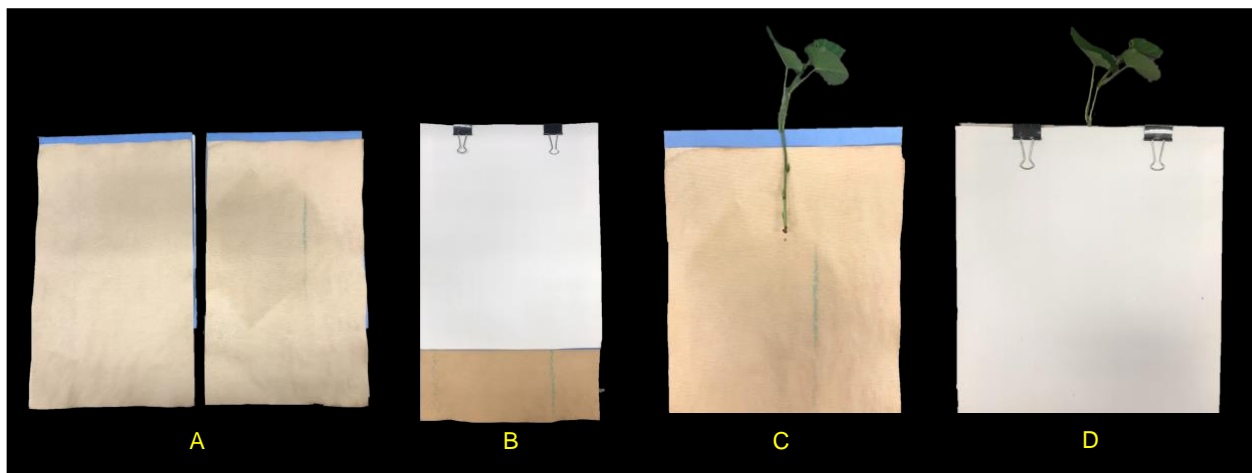
156 Each plant growth unit consisted of two sheets of heavy weight germination paper (18 in. H x 12
157 in. L, 76 lb., Anchor Paper Company, Saint Paul, MN, U.S.A.) followed by two sheets of Steel
158 Blue Seed germination paper (18 in. H x 12 in. L; 120 lb.; Anchor Paper Company, Saint Paul,
159 MN, U.S.A.) (Figure 3A). The germination paper was then sandwiched between two 0.157 in.
160 thick white corrugated plastic sheets (15 in. H x 12 in. L, Coroplast Inc. Chicago, IL, U.S.A.)
161 (Figure 3B) and then covered with 6 mm clear recycled polyethethylene sheeting (15 in. H x 12
162 in. L; HDX, Home Depot, Atlanta, GA). Four 1 ¼ in. metal binder clips (Staples, Framingham,
163 MA, U.S.A.) were used to attached and hold together the clear plastic sheeting around the white
164 corrugated plastic sheets. All germination paper was autoclaved (120 °C for 20 min) and plastic
165 sheeting was surface sterilized with 70% sodium hypochlorite and rinsed in deionized water.

166

167 **Growth unit assembly and stem ('slip') placement in growth unit**

168 With the rigid foam insulation lid covering the phenotyping system, each individual growth unit
169 with one protruding stem was positioned into one rectangular opening and secured from the top
170 with two 1 ¼ in. metal binder clips on each side (12 growth units per phenotyping system box).
171 One excised sweetpotato stem was used per individual growth unit (Figure 3C). In short, stems
172 from each genotype tested were randomly chosen and all mature leaves and petioles were
173 excised leaving only two to three small immature leaves at the top. Each stem was then cut to a
174 uniform length and care was taken so that two to three nodes were exposed and placed centered
175 into the growth unit (pre-moisten with nutrient solution) with the rest of the stem with leaves
176 protruding out (Figure 3D). Each growth unit was then closed and fastened with the metal binder
177 clips and hung through one rectangular slot of the phenotyping platform.

178



179

180 Figure 3. Individual growth units and 'slip' placement inside the growth unit: (A) left and right side of the
181 growth unit showing germination paper placement before 'slip' positioning, (B) closed and "sandwiched"
182 growth unit and secured with two metal binder clips (without 'slip'), (C) 'slip' placement in the middle of
183 one side of the growth unit and, (D) completed growth unit showing 'slip' protruding outward.

184

185

186

187 **Irrigation System (Ebb-and-Flow System)**

188 One 55-gallon heavy duty polypropylene tough tote with lid (45.43 in. L x 21.13 in. W x 19.52
189 in. H. HDX Model # HDX55GONLINE(4), Home Depot, Atlanta, GA, U.S.A.) was used as a
190 nutrient storage tank. The tank was equipped with one 1/12 HP submersible pump (Model: Little
191 Giant 4E-34NR Series; Franklin Electric Co., Inc., Fort Wayne, IN, U.S.A.). The pump was
192 connected to a flexible ½ in. male national pipe thread hose (MNPT hose). The hose was then
193 connected via an Ebb-and-Flow fitting kit (HydroFlow Products, Hawthorne Gardening Co.,
194 Vancouver, WA, U.S.A.) to one root phenotyping system. A digital timer was connected to the
195 pump system for periodic water supply. The nutrient solution consisted of: 7 mM N, 0.5 mM
196 P₂O₅; 7.5 mM K₂O; 2 mM Mg; 2 mM S; 50 µM B; 10 µM Mn; 5 µM Zn; 2 µM Cu; 1 µM Mo.
197 The nutrient solution stored in the nutrient supply tank was delivered to the phenotyping
198 platform via an automatic submersible pump through a time controller. The periodic pumping
199 was set as 10 min on and 240 min off during a 24-hour period. The nutrient solution was
200 refreshed weekly.

201

202 **Location, genotypes, and growth condition**

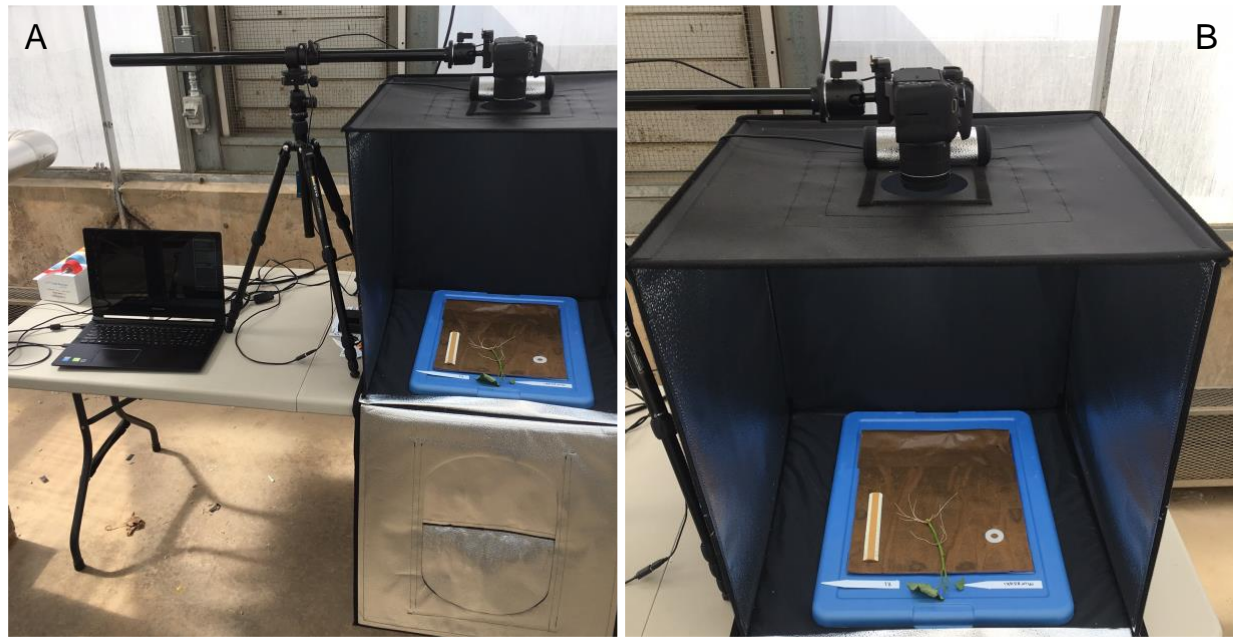
203 This study was conducted twice from September to October 2017 and from February to March
204 2018 in a temperature-controlled greenhouse at Penn State University located in University Park,
205 PA, USA (40°48'N, 77°51'W). Greenhouse environmental growth conditions exhibited a
206 photoperiod of 14/10 h at 32/28 °C (light/darkness) with a maximum midday photosynthetic flux
207 density of 1200 µmol photons m⁻² supplemented with LED lights. The ambient humidity was
208 40%. One commercial and commonly available sweetpotato clone, 'Covington', and one
209 unreleased breeder line, 'NC10-275', were tested throughout the system establishment of this
210 root phenotyping platform.

211

212 **Data collection**

213 Root growth was monitored, photographed, and measured every five days for a total of 20 days.
214 With care, each growth unit was removed from the phenotyping platform and opened by
215 removing the polyethethylene sheeting and white corrugated plastic sheets. Each growth unit was
216 placed centered inside a light tent with built-in LED lights (Angler) and photographed with a
217 standard DSLR camera (Canon; image size: 4000 x 6000 pixels; image DPI: 70 pixels/inch;
218 color model: RGB; file type: JPEG) positioned on an adjustable overhead camera platform
219 (Glide Gear) (Figure 4A and 4B). To account for root image scaling, a ruler was placed
220 alongside each root.

221



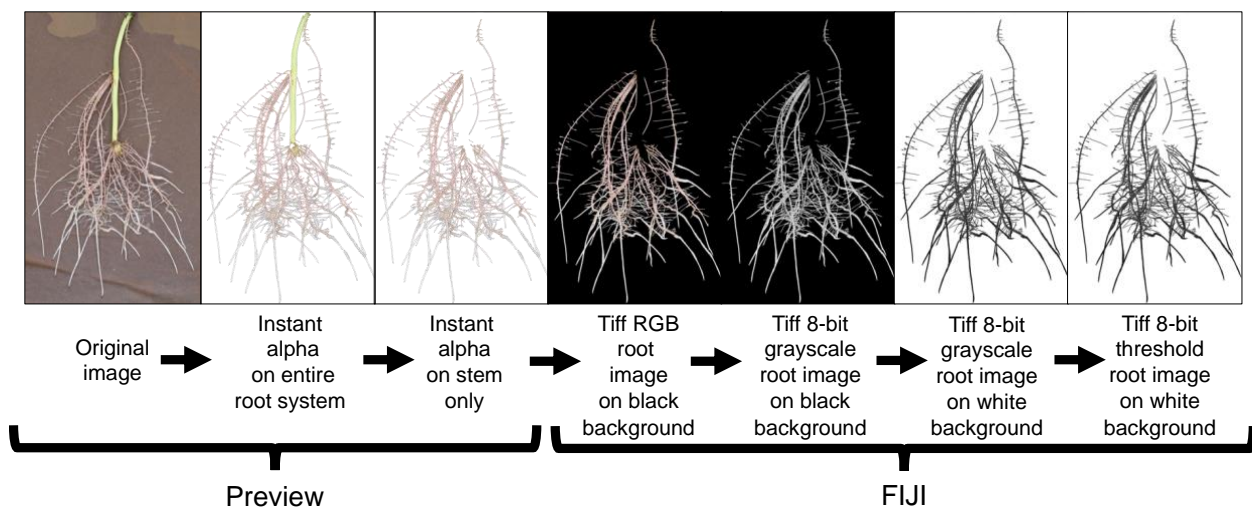
222
223 Figure 4. Imaging and data acquisition platform: (A) PC laptop connected to a standard DSLR digital
224 camera positioned on an adjustable platform, and (B) light tent with built in LED lights showing the
225 detail of the opened growth unit and exposing the 'slip' and root growth after 5 days.
226

227

227 Image Analysis

228 All root images were pre-processed using Preview (Version 10.0; Apple Inc. Cupertino, CA,
229 U.S.A.) and FIJI (Version 2.0.0-rc-69/1.52i; LOCI; University of Wisconsin-Madison, WI,
230 U.S.A.). Preview was used to crop and remove the stem (i.e., stem/slip) segment from the rest of
231 the root system using the *instant alpha* tool (Figure 5). This process was done manually to all
232 root images. Cropped images were loaded to FIJI and 32-bit RGB (red, green, blue) images were
233 converted to 8-bit grayscale LUT (look-up-table) for further processing. FIJI's *subtract*
234 *background* and *threshold* commands were then applied to separate roots from background
235 (Figure 5).
236

237



238

238 Figure 5. Root image processing sequence for subsequent root analysis in WinRhizo. This image
239 preparation method includes a cropping of the background germination paper and stem using the Instant

239

240 Alpha tool in Preview and then transferring the processed image to FIJI for image conversion and
241 thresholding.

242

243 Root Image Descriptors

244 For root morphological descriptors, WinRHIZO (V.2009 Pro, Regent Instruments, Montreal,
245 QC, Canada) was used to detect root structures from each image. The diameter classes were set
246 at 200 μm , the equivalent of two pixel with 10 equal intervals. The debris removal filter of
247 WinRHIZO was set to remove objects with an area smaller than 0.02 cm^2 and a length:width
248 ratio lower than 10. WinRHIZO was able to distinguish adventitious/nodal and lateral roots in all
249 images analyzed. All root morphological traits measured are listed in Table 1.

250

251 Table 1. Description of 10 measured traits for both sweetpotato genotypes grown in the root phenotyping
252 platform evaluated at 5, 10, 15 and 20 days after placement in the growth unit.

Trait Name	Unit	Trait Description
Total Root Length	cm	Cumulative length of all roots in entire root system
Total Root Surface Area	cm^2	Cumulative surface area of all roots in entire root system
Average Root Diameter	mm	Average diameter of all roots in entire root system
Total Root Volume	cm^3	Cumulative volume of all roots in entire root system
Number of Root Tips	count	Cumulative tips of all roots in entire root system
Number of Root Forks	count	Cumulative forks of all roots in entire root system
Root Length Pattern	cm	Root length by depth at each 10 cm depth
Root Depth Index	%	Percent vertical centroid of root distribution in the soil
Root Branching Density	branch cm^{-1}	Number of lateral branches per length unit along a root
Root Length Distribution by Diameter Class	cm	Cumulative root length by root diameter [very fine (0-0.6 mm), fine (>0.6 to \leq 1.2 mm), large (>1.2 to \leq 1.8 mm), and very large (>1.8 mm)]

253

254 Statistical Analysis

255 Analysis of variance was performed using JMP Pro 16 (SAS Institute, Cary, NC) on all
256 measured root traits. Data were transformed, when necessary, before ANOVA to achieve
257 normality. Tukey's Honest Significant Difference test was used to identify significant differences
258 among means. Statistical significance was based on a p value of < 0.05 .

259

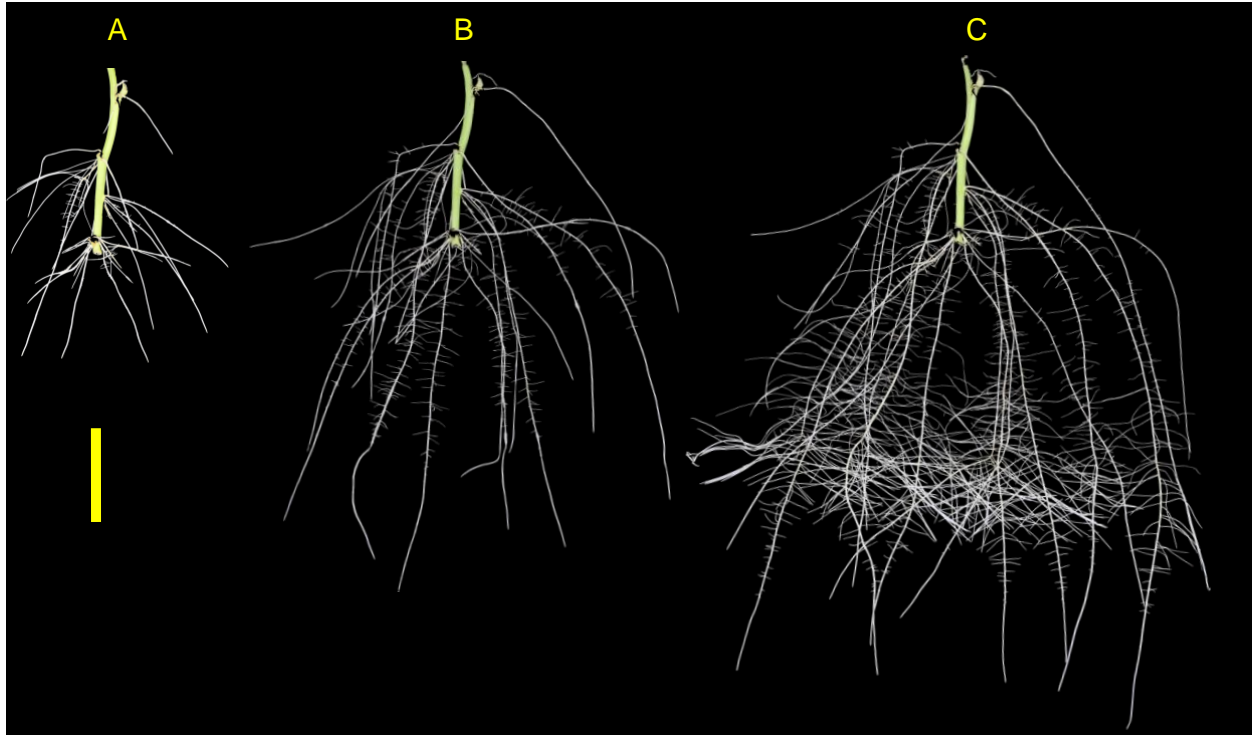
260 Results

261

262 Root development in the system

263 The root development for both genotypes tested were vigorous and presented root phenotype
264 variation within the phenotyping system. The root systems of both 'Covington' and 'NC10-275'
265 consisted of several first-order adventitious roots (i.e., lateral roots) originating from nodes
266 placed with the phenotyping system and by the end of the experiment, second-order root
267 branching was also observed (Figure 6).

268



269
270 Figure 6. Example images showing root morphology and development of 'NC10-275' grown in the root
271 phenotyping platform. Images were taken at (A) 5, (B) 10, and (C) 15 days after planting (scale bar = 10
272 cm).

273
274 **Root phenotype variation**

275 Phenotyping of both sweetpotato genotypes produced root systems that were imaged and
276 assessed every five days until day 20. Variations in several root traits between both genotypes
277 were substantial. Significant variations were detected after day 10 in total root length (CV = 0.24
278 to 0.33, total root surface area (CV = 0.28 to 0.31), total root volume (CV = 0.07 to 0.32), and
279 number of tips (CV = 0.22 to 0.48). After day 20, all root traits differed significantly for both
280 genotypes (Table 2). Specifically, 'NC10-275' had a higher total root length, greater total surface
281 root area, and larger total root volume compared to 'Covington'. However, on average
282 'Covington' had a larger root diameter compared to 'NC10-275' on every sampling day (Table
283 2).

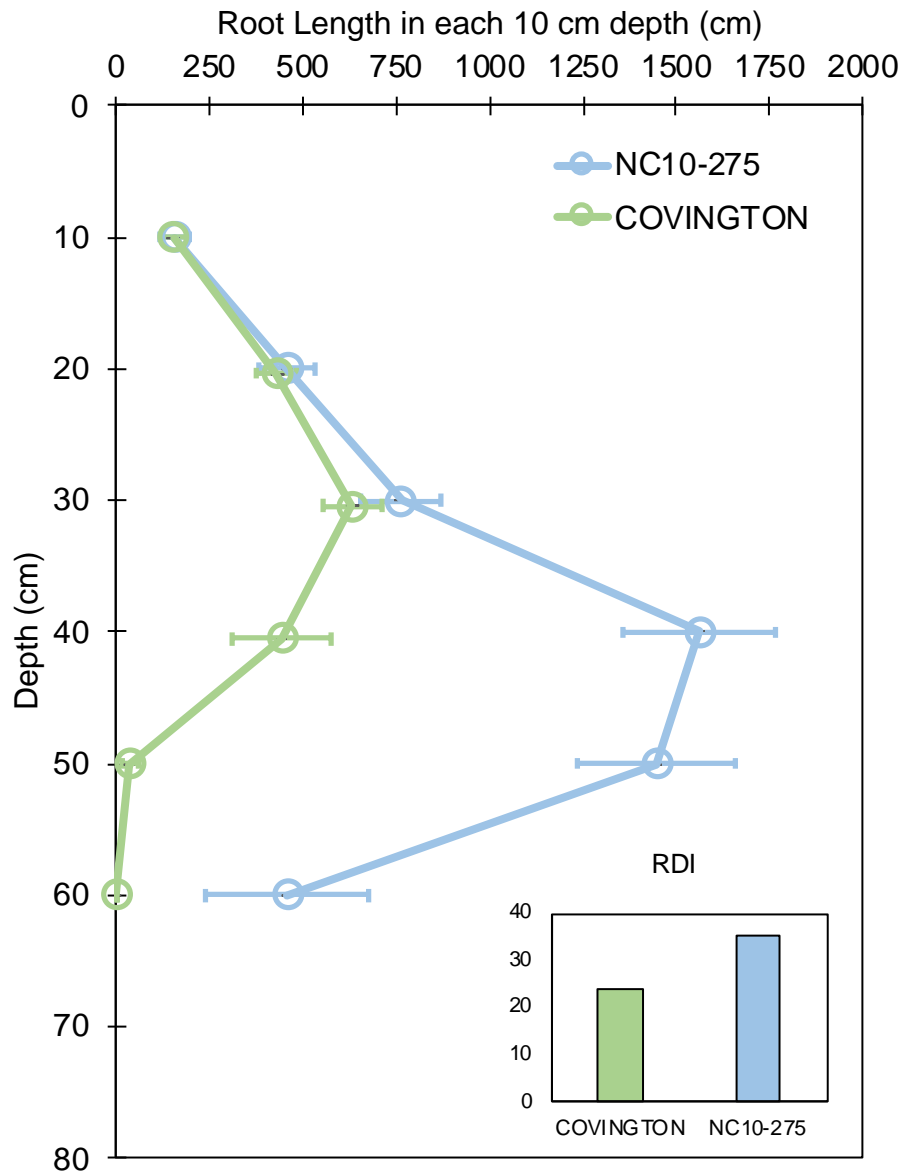
284
285 Table 2. Descriptive statistics of six measured root traits in 'Covington' and 'NC10-275' grown in a 2D
286 semi-hydroponic phenotyping platform assessed every five days until day 20.

Genotype	Trait	Unit	DAY 5					DAY 10					DAY 15					DAY 20				
			Min	Max	Mean	CV	Sig	Min	Max	Mean	CV	Sig	Min	Max	Mean	CV	Sig	Min	Max	Mean	CV	Sig
COVINGTON	Total Root Length	cm	20.3	77.8	44.1	0.44	<i>d</i>	122.2	276.4	183.9	0.33	<i>cd</i>	341.1	621.8	433.9	0.22	<i>bc</i>	600.0	1164.3	767.9	0.25	<i>b</i>
	Total Root Surface Area	cm ²	2.2	7.2	4.1	0.46	<i>d</i>	8.8	19.7	13.2	0.31	<i>cd</i>	25.4	53.3	36.7	0.24	<i>bc</i>	39.2	76.4	51.4	0.25	<i>b</i>
	Average Root Diameter	mm	0.4	1.3	1.0	0.28	<i>a</i>	0.6	0.8	0.7	0.09	<i>abcd</i>	0.7	0.9	0.8	0.06	<i>abc</i>	0.6	0.8	0.7	0.12	<i>cd</i>
	Total Root Volume	cm ³	0.1	0.8	0.3	0.68	<i>d</i>	0.5	1.1	0.7	0.32	<i>cd</i>	1.5	3.6	2.4	0.26	<i>bc</i>	1.9	3.9	2.7	0.29	<i>b</i>
	Number of Tips	-	44.0	274.0	106.6	0.80	<i>d</i>	180.0	761.0	386.6	0.48	<i>cd</i>	315.0	543.0	419.0	0.21	<i>c</i>	564.0	986.0	725.3	0.22	<i>b</i>
	Number of Forks	-	31.0	464.0	161.6	0.94	<i>c</i>	374.0	1268.0	657.0	0.47	<i>bc</i>	621.0	1617.0	1100.3	0.35	<i>bc</i>	1146.0	2894.0	1772.0	0.36	<i>b</i>
NC10-275	Total Root Length	cm	108.5	217.2	162.8	0.25	<i>cd</i>	556.0	1045.4	737.9	0.24	<i>b</i>	1106.9	2598.9	1862.7	0.23	<i>a</i>	1338.8	2646.2	2074.7	0.19	<i>a</i>
	Total Root Surface Area	cm ²	28.0	64.9	46.4	0.29	<i>cd</i>	97.5	210.4	148.0	0.28	<i>b</i>	162.9	530.3	361.7	0.30	<i>a</i>	220.6	569.8	390.2	0.28	<i>a</i>
	Average Root Diameter	mm	0.7	1.2	0.9	0.17	<i>ab</i>	0.6	0.7	0.6	0.07	<i>d</i>	0.5	0.7	0.6	0.11	<i>d</i>	0.5	0.7	0.6	0.15	<i>d</i>
	Total Root Volume	cm ³	0.6	1.6	1.1	0.38	<i>abcd</i>	1.4	3.7	2.4	0.32	<i>bc</i>	1.9	8.6	5.6	0.36	<i>a</i>	2.9	10.5	6.0	0.41	<i>a</i>
	Number of Tips	-	66.0	457.0	192.6	0.62	<i>cd</i>	587.0	1107.0	744.5	0.22	<i>b</i>	892.0	1800.0	1201.8	0.24	<i>a</i>	1091.0	1958.0	1472.6	0.19	<i>a</i>
	Number of Forks	-	116.0	658.0	330.9	0.61	<i>c</i>	1124.0	2359.0	1672.1	0.29	<i>b</i>	2295.0	7488.0	4440.2	0.35	<i>a</i>	3223.0	6482.0	5084.0	0.24	<i>a</i>

287
288 Traits with coefficients of variation (CVs) ≥ 0.3 appear in bold type. Means within a column followed by the
289 same letter (a to d) are not significantly different at $p < 0.05$, according to Tukey's HSD.

291 Root Length Pattern and Root-Depth Index

292 Root length by depth between ‘Covington’ and ‘NC10-275’ was non-significant from 0 to 30
293 cm, however significantly different from 30 to 50 cm by day 20 (Figure 7). Specifically,
294 ‘Covington’ displayed the largest portion of root length from 20-30 cm (37.3%), followed by 30-
295 40 cm (26.2%) and 10-20 cm (25.4%). Whereas ‘NC10-275’ exhibited the largest portion of root
296 length at 30-40 cm (32.2%) followed by 40-50 cm (29.8%) and 20-20 cm (15.8%). Lastly,
297 ‘NC10-275’ showed a total higher root-depth index (35.4%) compared to ‘Covington’ (23.6%).

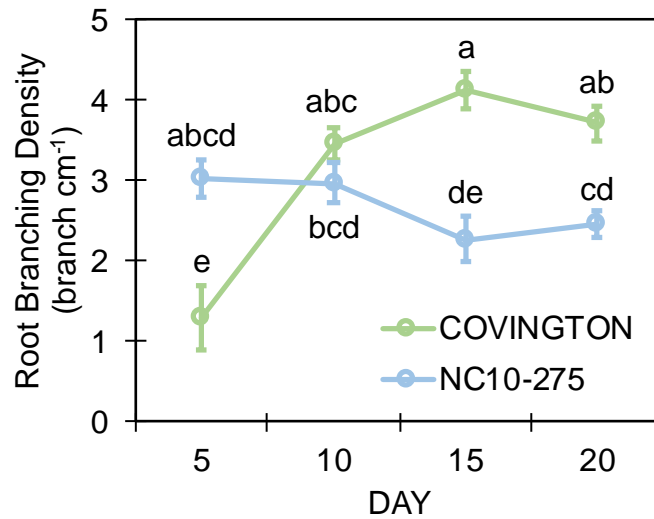


298 Figure 7. Root length in each 10 cm depth by soil depth and root depth index of ‘Covington’ and ‘NC10-
299 275’ sampled at day 20. Data shown are means ± SE of 12 replicates of the two genotypes.
300

301 Root Branching Density

302 Both genotypes selected for this study showed different lateral root branching density
303 phenotypes when compared at each sampling day (Figure 8). Under the phenotyping platform,
304 ‘Covington’ displayed a lower lateral root branching density compared to ‘NC10-275’ at day 5,
305

306 however, this trend changed by day 10 until the end of the experiment. By day 10, both
307 'Covington' and 'NC10-275' presented similar lateral root branching density quantities, although
308 by day 15 and 20, 'Covington' had significantly greater lateral root branching density when
309 compared to 'NC10-275'.
310



311
312 Figure 8. Lateral root branching density of adventitious roots at each sampling day for 'Covington' and
313 'NC10-275'. Data shown are means of 12 replicates of the two genotypes in each sampling day. Different
314 letters (a to d) represent significant differences at $p < 0.05$, according to Tukey's HSD
315

316 Root Length Distribution by Diameter Class

317 The total root length was divided into four diameter classes: very fine (0-0.6 mm), fine (>0.6 to
318 ≤ 1.2 mm), large (>1.2 to ≤ 1.8 mm), and very large (>1.8 mm). In general, the root length
319 distribution by diameter class of 'NC10-275' was significantly larger when compared to
320 'Covington' at each sampling day (Figure 9A and 9B). Specifically, the very fine and fine root
321 length of 'NC10-275' was greater than that of 'Covington' at day 5 (very fine: 56.9 cm
322 compared to 18.9 cm; fine: 95.3 cm compared to 14.5 cm), day 10 (very fine: 427.3 cm
323 compared to 94 cm; fine: 312.4 cm compared to 78.3 cm), day 15 (very fine: 995.2 cm compared
324 to 180.7 cm; fine: 531.4 cm compared to 157.9), and day 20 (very fine: 1184.9 cm compared to
325 429.7 cm; fine: 541.5 cm compared to 240.9 cm) respectively. Overall, the very fine and fine
326 root diameter classes represented the longest root length for both 'NC10-275' and 'Covington'
327 (97.7% and 92.4% of the total length) respectively. There was small to no significant differences
328 in root length distribution for large to very large root diameters between genotypes (Figure 9A
329 and 9B).

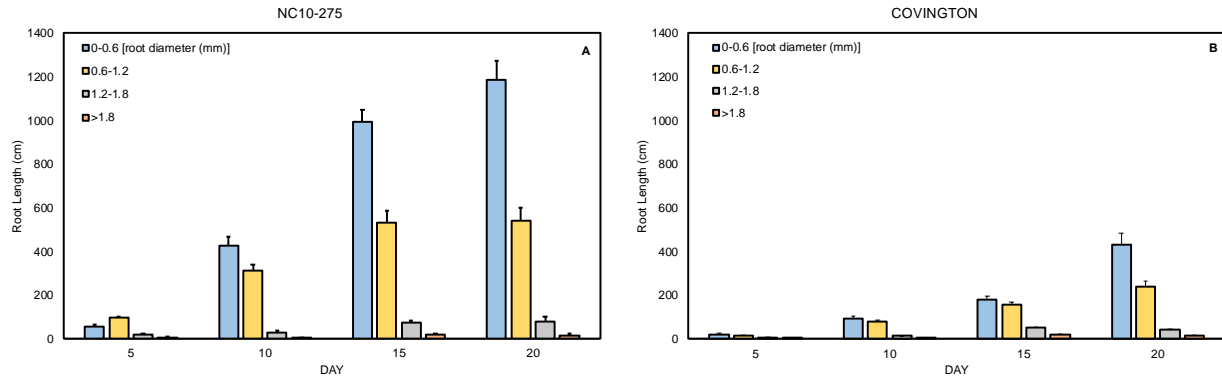


Figure 9. Mean root length distribution by diameter class of (A) 'NC10-275' and (B) 'Covington' at each sampling day. Data shown are means of 12 replicates of the two genotypes in each sampling day.

Discussion

The main reasons for developing this study were two-fold: first, to development a cheap, cost-effective, and efficient phenotyping system for examining stem-derived (i.e., adventitious/nodal) roots and second, to examine the inherent genetic variations in root traits among a commercially available sweetpotato clone and an unreleased breeder line. The combination of these two approaches could provide the basis for future root models and facilitate three-dimensional root architecture for selecting superior root traits for sweetpotato breeding programs worldwide. This experiment using sweetpotato was devised to test the efficiency of the phenotyping system and the performance of cut and prepared 'slips' in the system. The results of this pilot study will provide information for future follow-up screening experiments using the same plant species. The rationale for the use of sweetpotato, considered a root and tuber crop (RTC) model organism is that this root crop species (as well as other RTCs), have lingered behind the well-studied "model" crop species like maize, rice, soybean, and wheat, where the knowledge of RSA has already led to considerable advances in the ability of these crops to exploit soil resources under low-input conditions.

The root growth phenotyping platform described here conforms to a 'soilless 2D root phenotyping platform' that uses a semi-hydroponic medium similar to many published reports (Chen *et al.*, 2022; Adu *et al.*, 2014; Chen *et al.*, 2011; Le Marie *et al.*, 2014). Specifically, the phenotyping platform allowed for a clear visualization of sweetpotato stem-derived adventitious roots growing on each of the individual growth units. In addition, the platform allowed for the growing of eight 'slips' simultaneously that could be removed individually every five days for imaging. The root growth phenotyping platform is comparable to the 'pouch-and-wick' system that allows for an *in situ* observation of adventitious roots based on germination paper. We developed this system because it is affordable, expandable, simple to operate, and can be used to evaluate early RSA with high efficacy. Also, as the system is expandable, it can conform to increased repetitions if necessary. However, attention is needed when removing the individual growth units for imaging as sweetpotato's root system are fragile and root damage may occur. During root imaging, each individual growth unit was maintained moist and exposure time minimal to avoid roots from drying out. Per our observations, the root growth phenotyping platform is both semi-hydroponic and semi-aeroponic, which builds on the advantages of a strict hydroponic or aeroponic system. Since the root growth phenotyping platform uses an external and independent irrigation system (ebb-and-flow system) connected to each root growth unit,

367 nutrient solutions can be prepared and re-stocked minimizing disruptions to the root growth unit.
368 That said, this root growth phenotyping platform has the potential for root plasticity studies
369 under water and nutrient stress. To our knowledge, is the first report of an *in situ* soilless 2-D
370 root growth phenotyping system used on sweetpotato ‘slips’.

371
372 ‘NC10-275’ is an unreleased breeder line that is considered “drought or wilt tolerant” and mainly
373 used by the Sweetpotato Breeding and Genetics Program at North Carolina State University as a
374 parental line to exploit its abiotic stress tolerance for breeding ornamental sweetpotato (*pers.*
375 *comm*), whereas ‘Covington’ is one of the most important commercial sweetpotato grown in the
376 United States characterized by high yields and quality. The root systems of both ‘Covington’ and
377 ‘NC10-275’ revealed unique root morphological features and root traits when developed in the
378 root growth phenotyping platform. The root system of each genotype maintained comparable
379 growth patterns until after day 5. We compared images and data from each sampling day
380 between both genotypes and determined that after day 20 both root systems presented a higher
381 diversity of root traits compared earlier sampling days. Differences in root traits after day 10
382 included root length, surface root area, root diameter, root volume, root depth, and root
383 branching density. For example, it was noted that ‘NC10-275’ grew at a faster pace compared to
384 ‘Covington’ increasing the abovementioned traits in favor of ‘NC10-275’. However, average
385 root diameter and root branching density was higher in ‘Covington’. Also, it is noteworthy that
386 the root length distribution by diameter class of ‘NC10-275’ was greater in all instances
387 measured. Root length pattern was increased only after 30 cm depth (measured at day 20) for
388 both genotypes, yet after 30 cm depth ‘NC10-275’ expanded its root length exceeding that of
389 ‘Covington’. Taken as a whole, all root traits measured revealed contrasting differences between
390 both genotypes examined. ‘NC10-275’ exhibited an earlier root growth habit with more deeply
391 distributed root system than ‘Covington’, probably due to its inherent drought tolerance where
392 roots present a more vertical growth pattern. In contrast, ‘Covington’ revealed an overall reduced
393 root volume, higher root branching density, and larger average diameter roots. This phenomenon
394 could be explained from the basis on current agricultural management practices where fertilizer
395 and water supply are abundant lessening the burden of root exploration for soil nutrients and
396 water and investing more resources in storage root formation and swelling. These results could
397 be confirmed by the higher root depth index (RDI) of the ‘NC10-275’, echoing the deeper root
398 system of this genotype. Though root spreading (root width growth) was not accounted for,
399 together with root depth pattern and root depth index are key traits for soil exploration for
400 improving the acquisition of limiting resources. Regardless of both genotypes belonging to the
401 same species (*I. batatas*), these results ratify the contrast that can be found between sweetpotato
402 root systems. It is notable that no previous studies on the RSA or root traits of both ‘Covington’
403 and NC10-275 have been published. Nevertheless, the first published report measuring lateral
404 root branching in sweetpotato was in 1949 ([Koshimizu and Nishida, 1949](#)), followed by other
405 published reports years later ([Villordon et al., 2012](#); [Pardales and Yamauchi, 2003](#)).

406
407 Though this research did not account for specific abiotic stress treatments [e.g., nitrogen (N),
408 phosphorus (P), potassium (K) deficiencies, and/or water stress]] within the root growth
409 phenotyping platform, there are now several published reports on the effects of N, P, K, and B
410 deficiencies on RSA and root traits using mesocosms filled with sand or other substrates. For
411 example, Villordon et al. ([2013](#)) demonstrated that lateral root branching jointly measured as
412 lateral root length, number of lateral roots and lateral root density in ‘Beauregard’ was altered in

413 response to variation in overall available N. Also, Villordon et al. (2020) revealed the existence
414 of genetic variation for inorganic P efficiency in ‘Bayou Belle’, ‘Beauregard’ and ‘Orleans’
415 sweetpotato cultivars by measuring root lateral root number and lateral root density and found
416 that these two root traits have been indirectly selected for inbreeding programs that focus on
417 early storage root formation and stable yields across environments. Furthermore, Liu et al.
418 (2017) showed differences in root length, surface area, root volume and average root diameter
419 under controlled K and deficient K using two cultivars, Ningzishu 1 (sensitive to K deficiency)
420 and Xushu 32 (tolerant to K deficiency). These results suggest potential genotypic differences in
421 RSA and K absorption ability under K deficiency. Likewise, Wang et al. (2017), showed that
422 increased K improved total root length, average root diameter and significantly increased the
423 differentiation from adventitious roots to fibrous roots and tuberous roots. These root traits
424 coupled with additional K could be beneficial to the increased number of storage roots per plant,
425 early formation of storage roots, root biomass, and overall yield. Under differing B availability,
426 Villordon and Gregorie (2021) showed evidence of cultivar-specific responses for reduced lateral
427 root length, root length, and reduced storage root swelling in ‘Beauregard’, ‘Murasaki’, and
428 ‘Okinawa’ cultivars.

429

430 **Conclusions**

431 Root growth patterns for both genotypes tested retained comparable growth patterns until after
432 five days in the phenotyping platform. After 20 days in the phenotyping platform both root
433 systems showed the highest diversity and difference of root traits compared to earlier sampling
434 days. Root length, surface root area, root volume, and root depth were higher in ‘NC10-275’.
435 Average root diameter and root branching density were higher in ‘Covington’. Sweetpotato is a
436 clonally propagated crop, sexual seeds are not used for planting, hence the experiment was
437 performed with ‘slips’, the central unit of sweetpotato planting material used routinely in the
438 field. In summary, this is the first report of a phenotyping system that uses a stem and not a
439 sexual seed as starting material. This experiment confirmed genotypic variations in the early root
440 system growth of sweetpotato using an ebb and flow soilless phenotyping platform. This
441 phenotyping study was reproducible across the whole growing period and for both genotypes
442 tested. However, one of the potential drawbacks of this system is the early inference of the
443 potential performance of these genotypes in the field. Thus, under changing growing
444 environments, roots may present specific responses making their inherent phenotypic plasticity
445 critical for mining edaphic resources (Lynch *et al.*, 2021). Yet, it is still possible to extrapolate
446 early genotypic differences between sweetpotato germplasm and phenotypic plasticity under
447 imposed stress treatments.

448

449 **Acknowledgements**

450 The corresponding author would like to thank Dr. Jonathan Lynch (Penn State University) and
451 Dr. Craig Yencho (North Carolina State University) for guidance.

References

- Adu, M. O., Chatot, A., Wiesel, L., Bennett, M. J., Broadley, M. R., White, P. J. & Dupuy, L. X. (2014). A scanner system for high-resolution quantification of variation in root growth dynamics of *Brassica rapa* genotypes. *Journal of Experimental Botany* 65(8): 2039-2048.
- Anami, S. E., Zhang, L. M., Xia, Y., Zhang, Y. M., Liu, Z. Q. & Jing, H. C. (2015). Sweet sorghum ideotypes: genetic improvement of the biofuel syndrome. *Food and Energy Security* 4(3): 159-177.
- Blossfeld, S., Le Marie, C. A., Van Dusschoten, D., Suessmilch, S. & Kuhn, A. J. (2011). Non-invasive investigation of root growth via NMR imaging. *Commun Agric Appl Biol Sci* 76(2): 11-13.
- Burridge, J., Jochua, C. N., Bucksch, A. & Lynch, J. P. (2016). Legume shovelomics: High-Throughput phenotyping of common bean (*Phaseolus vulgaris* L.) and cowpea (*Vigna unguiculata* subsp. *unguiculata*) root architecture in the field. *Field Crops Research* 192: 21-32.
- Chen, X. Y., Liu, P., Zhao, B., Zhang, J. W., Ren, B. Z., Li, Z. & Wang, Z. Q. (2022). Root physiological adaptations that enhance the grain yield and nutrient use efficiency of maize (*Zea mays* L.) and their dependency on phosphorus placement depth. *Field Crops Research* 276.
- Chen, Y. L., Dunbabin, V. M., Diggle, A. J., Siddique, K. H. M. & Rengel, Z. (2011). Development of a novel semi-hydroponic phenotyping system for studying root architecture. *Functional Plant Biology* 38(5): 355.
- Clark, R. T., Famoso, A. N., Zhao, K. Y., Shaff, J. E., Craft, E. J., Bustamante, C. D., McCouch, S. R., Aneshansley, D. J. & Kochian, L. V. (2013). High-throughput two-dimensional root system phenotyping platform facilitates genetic analysis of root growth and development. *Plant Cell and Environment* 36(2): 454-466.
- Clark, R. T., MacCurdy, R. B., Jung, J. K., Shaff, J. E., McCouch, S. R., Aneshansley, D. J. & Kochian, L. V. (2011). Three-Dimensional Root Phenotyping with a Novel Imaging and Software Platform. *Plant Physiology* 156(2): 455-465.
- de Dorlodot, S., Forster, B., Pages, L., Price, A., Tuberosa, R. & Draye, X. (2007). Root system architecture: opportunities and constraints for genetic improvement of crops. *Trends in Plant Science* 12(10): 474-481.
- Downie, H., Holden, N., Otten, W., Spiers, A. J., Valentine, T. A. & Dupuy, L. X. (2012). Transparent Soil for Imaging the Rhizosphere. *Plos One* 7(9).
- Fang, S. Q., Yan, X. L. & Liao, H. (2009). 3D reconstruction and dynamic modeling of root architecture in situ and its application to crop phosphorus research. *Plant Journal* 60(6): 1096-1108.
- Gao, Y. Z. & Lynch, J. P. (2016). Reduced crown root number improves water acquisition under water deficit stress in maize (*Zea mays* L.). *Journal of Experimental Botany* 67(15): 4545-4557.
- Gaudin, A. C. M., McClymont, S. A., Holmes, B. M., Lyons, E. & Raizada, M. N. (2011). Novel temporal, fine-scale and growth variation phenotypes in roots of adult-stage maize (*Zea mays* L.) in response to low nitrogen stress. *Plant Cell and Environment* 34(12): 2122-2137.
- Hammer, G. L., Dong, Z. S., McLean, G., Doherty, A., Messina, C., Schusler, J., Zinselmeier, C., Paszkiewicz, S. & Cooper, M. (2009). Can Changes in Canopy and/or Root System Architecture Explain Historical Maize Yield Trends in the US Corn Belt? *Crop Science* 49(1): 299-312.
- Hochholdinger, F., Park, W. J., Sauer, M. & Woll, K. (2004). From weeds to crops: genetic analysis of root development in cereals. *Trends in Plant Science* 9(1): 42-48.
- Hund, A., Reimer, R. & Messmer, R. (2011). A consensus map of QTLs controlling the root length of maize. *Plant and Soil* 344(1-2): 143-158.
- Hund, A., Trachsel, S. & Stamp, P. (2009). Growth of axile and lateral roots of maize: I development of a phenotyping platform. *Plant and Soil* 325(1-2): 335-349.
- Iyer-Pascuzzi, A. S., Symonova, O., Mileyko, Y., Hao, Y. L., Belcher, H., Harer, J., Weitz, J. S. & Benfey, P. N. (2010). Imaging and Analysis Platform for Automatic Phenotyping and Trait Ranking of Plant Root Systems. *Plant Physiology* 152(3): 1148-1157.
- Khan, M. A., Gemenet, D. & Villordon, A. (2016). Root System Architecture and Abiotic Stress Tolerance: Current Knowledge in Root and Tuber Crops. *Frontiers in Plant Science* 7.
- Koshimizu, T. & Nishida, M. (1949). On the relation between the distribution of free-auxin in the young sweet potato plant and its root-tuber formation. *Shokubutsugaku Zasshi* 62(735-736): 146-153.
- Kuijken, R. C. P., van Eeuwijk, F. A., Marcelis, L. F. M. & Bouwmeester, H. J. (2015). Root phenotyping: from component trait in the lab to breeding. *Journal of Experimental Botany* 66(18): 5389-5401.
- Le Marie, C., Kirchgessner, N., Flutsch, P., Pfeifer, J., Walter, A. & Hund, A. (2016). RADIX: rhizoslide platform allowing high throughput digital image analysis of root system expansion. *Plant Methods* 12.

- Le Marie, C., Kirchgessner, N., Marschall, D., Walter, A. & Hund, A. (2014). Rhizoslides: paper-based growth system for non-destructive, high throughput phenotyping of root development by means of image analysis. *Plant Methods* 10.
- Liu, M., Zhang, A. J., Chen, X. G., Jin, R., Li, H. M. & Tang, Z. H. (2017). Effects of potassium deficiency on root morphology, ultrastructure and antioxidant enzyme system in sweet potato (*Ipomoea batatas* [L.] Lam.) during early growth. *Acta Physiologiae Plantarum* 39(9).
- Lynch, J. (1995). Root Architecture and Plant Productivity. *Plant Physiology* 109(1): 7-13.
- Lynch, J. P., Strock, C. F., Schneider, H. M., Sidhu, J. S., Ajmera, I., Galindo-Castaneda, T., Klein, S. P. & Hanlon, M. T. (2021). Root anatomy and soil resource capture. *Plant and Soil* 466(1-2): 21-63.
- Metzner, R., Eggert, A., van Dusschoten, D., Pflugfelder, D., Gerth, S., Schurr, U., Uhlmann, N. & Jahnke, S. (2015). Direct comparison of MRI and X-ray CT technologies for 3D imaging of root systems in soil: potential and challenges for root trait quantification. *Plant Methods* 11.
- Nagel, K. A., Putz, A., Gilmer, F., Heinz, K., Fischbach, A., Pfeifer, J., Faget, M., Blossfeld, S., Ernst, M., Dimaki, C., Kastenholz, B., Kleinert, A. K., Galinski, A., Scharr, H., Fiorani, F. & Schurr, U. (2012). GROWSCREEN-Rhizo is a novel phenotyping robot enabling simultaneous measurements of root and shoot growth for plants grown in soil-filled rhizotrons. *Functional Plant Biology* 39(10-11): 891-904.
- Pace, J., Lee, N., Naik, H. S., Ganapathysubramanian, B. & Lubberstedt, T. (2014). Analysis of Maize (*Zea mays* L.) Seedling Roots with the High-Throughput Image Analysis Tool ARIA (Automatic Root Image Analysis). *Plos One* 9(9).
- Pardales, J. R. & Yamauchi, A. (2003). Regulation of root development in sweetpotato and cassava by soil moisture during their establishment period. In *Roots: The Dynamic Interface between Plants and the Earth.*, 201-208. New York, NY, U.S.A.: Springer.
- Pflugfelder, D., Metzner, R., van Dusschoten, D., Reichel, R., Jahnke, S. & Koller, R. (2017). Non-invasive imaging of plant roots in different soils using magnetic resonance imaging (MRI). *Plant Methods* 13.
- Purushothaman, R., Krishnamurthy, L., Upadhyaya, H. D., Vadez, V. & Varshney, R. K. (2017a). Genotypic variation in soil water use and root distribution and their implications for drought tolerance in chickpea. *Functional Plant Biology* 44(2): 235-252.
- Purushothaman, R., Krishnamurthy, L., Upadhyaya, H. D., Vadez, V. & Varshney, R. K. (2017b). Root traits confer grain yield advantages under terminal drought in chickpea (*Cicer arietinum* L.). *Field Crops Research* 201: 146-161.
- Rascher, U., Blossfeld, S., Fiorani, F., Jahnke, S., Jansen, M., Kuhn, A. J., Matsubara, S., Martin, L. L. A., Merchant, A., Metzner, R., Muller-Linow, M., Nagel, K. A., Pieruschka, R., Pinto, F., Schreiber, C. M., Temperton, V. M., Thorpe, M. R., van Dusschoten, D., van Volkenburgh, E., Windt, C. W. & Schurr, U. (2011). Non-invasive approaches for phenotyping of enhanced performance traits in bean. *Functional Plant Biology* 38(12): 968-983.
- Ribeiro, K. M., Barreto, B., Pasqual, M., White, P. J., Braga, R. A. & Dupuy, L. X. (2014). Continuous, high-resolution biospeckle imaging reveals a discrete zone of activity at the root apex that responds to contact with obstacles. *Annals of Botany* 113(3): 555-563.
- Saengwilai, P., Nord, E. A., Chimungu, J. G., Brown, K. M. & Lynch, J. P. (2014). Root Cortical Aerenchyma Enhances Nitrogen Acquisition from Low-Nitrogen Soils in Maize. *Plant Physiology* 166(2): 726-735.
- Siddique, K. H. M., Chen, Y. L. & Rengel, Z. (2015). Efficient root system for abiotic stress tolerance in crops. *Agriculture and Climate Change - Adapting Crops to Increased Uncertainty (Agri 2015)* 29: 295-295.
- Topp, C. N., Iyer-Pascuzzi, A. S., Anderson, J. T., Lee, C. R., Zurek, P. R., Symonova, O., Zheng, Y., Bucksch, A., Mileyko, Y., Galkovskyi, T., Moore, B. T., Harer, J., Edelsbrunner, H., Mitchell-Olds, T., Weitz, J. S. & Benfey, P. N. (2013). 3D phenotyping and quantitative trait locus mapping identify core regions of the rice genome controlling root architecture. *Proceedings of the National Academy of Sciences of the United States of America* 110(18): E1695-E1704.
- Tuberosa, R., Salvi, S., Sanguineti, M. C., Landi, P., MacCafferri, M. & Conti, S. (2002). Mapping QTLs regulating morpho-physiological traits and yield: Case studies, shortcomings and perspectives in drought-stressed maize. *Annals of Botany* 89: 941-963.
- Villordon, A. & Gregorie, J. C. (2021). Variation in Boron Availability Alters Root Architecture Attributes at the Onset of Storage Root Formation in Three Sweetpotato Cultivars. *Hortscience* 56(11): 1423-+.
- Villordon, A., Gregorie, J. C. & LaBonte, D. (2020). Variation in Phosphorus Availability, Root Architecture Attributes, and Onset of Storage Root Formation among Sweetpotato Cultivars. *Hortscience* 55(12): 1903-+.

- Villordon, A., LaBonte, D., Firon, N. & Carey, E. (2013). Variation in Nitrogen Rate and Local Availability Alter Root Architecture Attributes at the Onset of Storage Root Initiation in 'Beauregard' Sweetpotato. *Hortscience* 48(6): 808-815.
- Villordon, A., LaBonte, D., Solis, J. & Firon, N. (2012). Characterization of Lateral Root Development at the Onset of Storage Root Initiation in 'Beauregard' Sweetpotato Adventitious Roots. *Hortscience* 47(7): 961-968.
- WANG Shun-Yi, L. H., LIU Qing, SHI Yan-Xi* (2017). Effect of Potassium Application on Root Grow and Yield of Sweet Potato and Its Physiological Mechanism. *Acta Agronomica Sinica* 43(07): 1057-1066.
- Wasson, A. P., Richards, R. A., Chatrath, R., Misra, S. C., Prasad, S. V., Rebetzke, G. J., Kirkegaard, J. A., Christopher, J. & Watt, M. (2012). Traits and selection strategies to improve root systems and water uptake in water-limited wheat crops. *Journal of Experimental Botany* 63(9): 3485-3498.
- Watt, M., Moosavi, S., Cunningham, S. C., Kirkegaard, J. A., Rebetzke, G. J. & Richards, R. A. (2013). A rapid, controlled-environment seedling root screen for wheat correlates well with rooting depths at vegetative, but not reproductive, stages at two field sites. *Annals of Botany* 112(2): 447-455.
- Xie, Q., Fernando, K. M. C., Mayes, S. & Sparkes, D. L. (2017). Identifying seedling root architectural traits associated with yield and yield components in wheat. *Annals of Botany* 119(7): 1115-1129.
- Zhan, A. & Lynch, J. P. (2015). Reduced frequency of lateral root branching improves N capture from low-N soils in maize. *Journal of Experimental Botany* 66(7): 2055-2065.
- Zhan, A., Schneider, H. & Lynch, J. P. (2015). Reduced Lateral Root Branching Density Improves Drought Tolerance in Maize. *Plant Physiology* 168(4): 1603-U1885.